Steel and Composite Structures, *Vol. 27, No. 2 (2018) 135-147*
DOI: https://doi.org/10.12989/scs.2018.27.2.135

Experimental and numerical study on energy absorption of lattice-core sandwich beam

Hossein Taghipoor * and Mohammad Damghani Noori [a]

Department of Mechanical Engineering, Semnan University, Semnan, P.O.B. 35131-19111, Semnan, Iran

(*Received August 16, 2017, Revised January 11, 2018, Accepted February 20, 2018*)

Abstract. Quasi-static three-point bending tests on sandwich beams with expanded metal sheets as core were conducted. Relationships between the force and displacement at the mid-span of the sandwich beams were obtained from the experiments. Numerical simulations were carried out using ABAQUS/EXPLCIT and the results were thoroughly compared with the experimental results. A parametric analysis was performed using a Box-Behnken design (BBD) for the design of experiments (DOE) techniques and a finite element modeling. Then, the influence of the core layers number, size of the cell and, thickness of the substrates was investigated. The results showed that the increase in the size of the expanded metal cell in a reasonable range was required to improve the performance of the structure under bending collapse. It was found that core layers number and size of the cell was key factors governing the quasi-static response of the sandwich beams with lattice cores.

Keywords: bending and shear strength; energy dissipation; quasi-static; steel/steel structure; numerical analysis

1. Introduction

Energy absorption systems are used in many engineering applications, moving systems in particular, for preventing or reducing damage. Sandwich beams with lattice cores are commonly used as energy absorber elements in crashworthiness applications due to their excellent load-carrying capacity and energy absorbing characteristics. These elements are widely used in aerospace, naval, sporting and outomotive applications. Bending collapse of sandwich beams is one of the most important energy dissipation mechanisms since transverse impact loading is the most common case in the real accidental crash events. Nevertheless, the bending collapse of sandwich beams has been relatively less studied when compared to axial crushing. This may be due to the fact that the energy dissipation under axial crushing is about one order of magnitude greater than that of bending collapse.

Typical sandwich structures consist of two thin, stiff and strong face sheets separated by a lightweight core that is usually made of honeycomb or corrugated core. The core material keeps the face sheets in their relative positions in the sandwich with little increase in weight, to increase bending and buckling resistance, as it enhances shear stiffness and energy absorption ability (Gibson and Ashby 1997).

Failure modes (face sheet compressive failure, debonding, wrinkling, indentation failure, and core compressive or shear failure) depend on many factors, such as loading types, material properties and geometries of structures (Daniel *et al*. 2002, Crupi and Montanini 2007). For sandwich beams under compression, or in pure bending, if the core is much stiffer than the skin in the thickness direction, compressive failure of the skins occurs; otherwise, facing wrinkling takes place (Daniel *et al*. 2003). According to quasi-static bending test results, Li *et al*. (2006) proposed an elastic-plastic model to analyze the dynamic response of composite sandwich beams and the model characterized the bending responses in three regimes: namely, the elastic regime, core-crushing regime and final failure regime.

Quasi-static deformation behavior of sandwich beams are usually studied by conducting three point or four point bending tests (Zhu *et al*. 2010). Vaidya *et al*. (2015) simulated three-point bending responses of simply supported sandwich beams using ABAQUS. Xiang *et al*. (2015) studied the quasi-static three-point bending behavior of sandwich beams with a series of identical thin-walled tubes as core. They obtained relationships between the force and displacement at the mid-span of the sandwich beam from the experiments.

Sandwich structures with Y, Kagome, corrugated and tetragonal cores under compressive and shear loading were simulated and the compressive responses were explored in detail (Vaidya *et al*. 2015, Pedersen *et al*. 2006, Hyun *et al*. 2003).

Another attractive sandwich core is lattice materials (Hu *et al*. 2016). In recent years, expanded metal sheets have found prominent applications. These applications fall into three main areas: furniture, construction, and energy absorbing systems (Smith *et al*. 2009). Teixeira *et al*. (2016) studied the quasi-static shear response performance on expanded metal panels. They found that shear response

*Corresponding author, Ph.D.,
E-mail: hosseintaghipoor@semnan.ac.ir
[a] Associate Professor, E-mail: mnoori@semnan.ac.ir

http://www.techno-press.org/?journal=scs&subpage=6
ISSN: 1229-9367 (Print), 1598-6233 (Online)

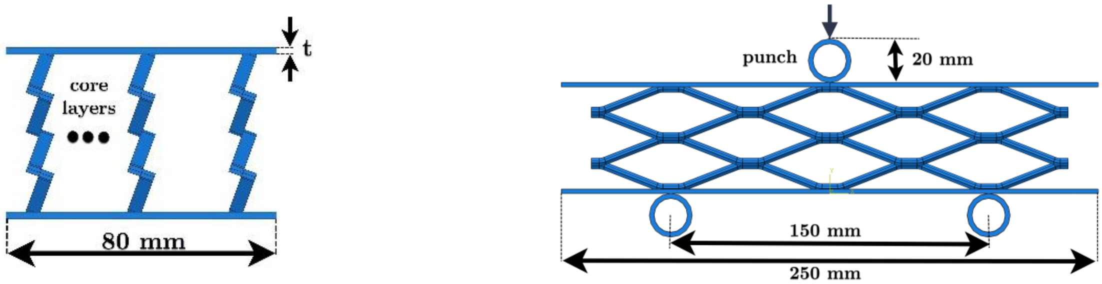

(a) (b)

Fig. 1 Geometry for simulation: (a) front view; and (b) side view

depends mainly on cell geometry and panel length, whereas the effect of the panel height is almost negligible. This property is used for plastic collapse. The collapse mechanism in latticed sheets is as follows: first, the cells start closing as the load increases, and plastic hinges are attained at nodal intersections. These plastic deformations gradually spread. The failure mechanism specifically appears as the plastic hinges at cell junctions. The force-displacement response curves show the gradual increase in the force, which is a favorable behavior for an energy absorbing system. This is because damping of the force must be gradual in these systems (Graciano *et al*. 2009; Smith *et al*. 2016, Nouri *et al*. 2015). Graciano *et al*. (2012) studied the axial collapse of circular tubes made of expanded metal sheets. Their test results showed that the collapse mechanism depended on cell direction and that the initial peak force depended on the number of cross-sectional cells (Graciano *et al*. 2012).

Jahromi and Hatami (2017) studied the Ea performance on multilayer expanded metal tubes under axial impact with using drop hammer test. They found that the tubes with zero degree angle cells had asymmetric collapse mechanism and increase in the size of the cells decreased the peak crushing force and Ea capacity. Hatami and Damghani Nouri (2015) presented the experimental and numerical investigation of a lattice-walled cylindrical shell. In their study, the type of collapse, force-displacement diagrams, crushing length, and absorbed energy were investigated. The experimental and numerical results were compared and it was observed that they were in good agreement (Hatami and Damghani Nouri 2015).

Deliberation of the response of sandwich beams to quasi-static loads is an equally necessary part of the complete structural design process. A detailed evaluation of the quasi-static performance of sandwich beams with lattice cores is necessary to attain a complete understanding of the structural response of such systems. To address this situation, the quasi-static response of sandwich beams with lattice cores is investigated by performing quasi-static tests on laboratory-scale specimens and covering finite element simulations to large-scale beam specimens.

In this study, a quasi-static loading protocol was employed, and the response of the absorber sandwich beams with expanded metal sheets as core under such loading was studied experimentally and numerically. A parametric analysis is performed using the design of experiments (DOE) techniques. DOE is an important and

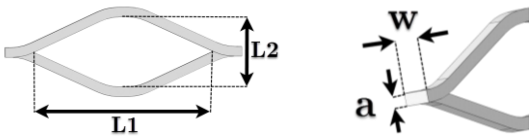

Fig. 2 Definition of geometric parameters of a cell of expanded metal sheets

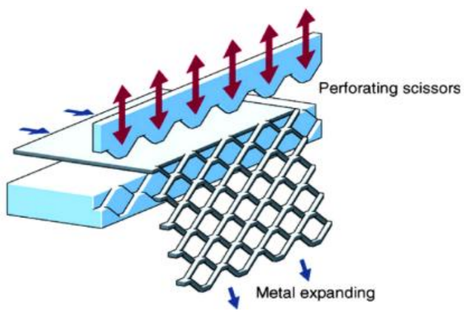

Fig. 3 Schematic of the manufacturing process for the expanded metal sheets (Kooistra and Wadley 2007)

beneficial tool for improvement and optimization of the production process and can play an important role in engineering design. Response surface method (RSM), as the subgroup of DOE techniques, can be helpful in finding optimum design variables in combination with multicriteria decision-making (MCDM) techniques. A Box-Behnken design (BBD) is elaborated for sampling design, then the influence of the geometry of the expanded metal cells, the thickness of face sheets and layer number of the core are investigated in depth. Thereafter, the energy absorption characteristics (peak load, mean load, energy absorbed, specific energy absorbed, and structural efficiency) are measured.

2. Materials and methods

The geometry and setup of the three-point bending test are shown in Fig. 1(a). Loaded by a cylinder punch, sandwich beams with lattice core were supported by two cylindrical supports. The sandwich beam with lattice core specimen (see Fig. 1) consisted of two substrates: the top substrate, which faced the load, and the bottom substrate, zwhich rested on the supports. Between the two substrates were arranged variable numbers of core layers, as shown in

Table 1 Dimensions of the expanded metal cells

Type	L_1 (mm)	L_2 (mm)	W (mm)	a (mm)	φ (mm^2)
1	15	7	1.5	0.9	0.081
2	34	11	2.2	1.5	0.145
3	64	22	4	3	0.562

Fig. 1(b). Both the substrates had the same dimensions, 80 mm (width), 250 mm (length), and three variables thickness (t). The substrates and core layers were made of the same material.

Fig. 3 schematically shows the slitting and expanding process of lattice sheets. The patterns in the expanded metal absorber were demonstrated by two parameters. L_2 denoted the lesser length, and L_1 denoted the greater length (Fig. 2). Table 1 shows the dimensions of the cells used herein (Graciano *et al*. 2012). Defined this plastic mechanism and proposed the following equation for the collapse load of a single expanded metal cell.

$$p = \frac{2\sigma_y w a^2}{L_1} \tag{1}$$

Where σ_y is the quasi-static yield stress; w is the strand width; α is the strand thickness and L_1 is the major axis. From Eq. (1), a parameter φ, that groups all the dimensions of the cell into one, is derived in order to investigate the influence of the cell geometry on to the energy absorber response (Borges *et al*. 2016).

$$\varphi = \frac{wa^2}{L_1} \tag{2}$$

Design variables and their ranges were selected based on the studying works of research. In this study, the ranges of the design variables are as follows

$$\begin{gathered} 3 \le N(core\ layers\ number) \le 9 \\ 0.081\ \text{mm}^2 \le \varphi\ (cell\ size) \le 0.562\ \text{mm}^2 \\ 1\ \text{mm} \le t(substrates\ thickness) \le 3\ \text{mm} \end{gathered} \tag{3}$$

For calculating energy absorption and shock resistance capability, the initial peak force (P_{peak}), the mean force (P_{mean}), the energy absorption capacity (E_a), specific energy absorption (SEA), and crushing force efficiency (CFE) selected as design goals (Eqs. (4)-(7)). Energy absorbed per unit weight (SEA), are important in system design, where, weight is the constraining factor. The amount of the absorbed energy is the area under the force-displacement curve. The crushing force efficiency is the ratio of the mean force to the initial peak force.

$$E_a = \int_0^{\delta_{\max}} F(\delta)d\delta \tag{4}$$

$$P_{mean} = \frac{1}{\delta_{\max}} \int_0^{\delta_{\max}} F(\delta)d\delta \tag{5}$$

$$CFE = \frac{P_{mean}}{P_{peak}} \times 100 \tag{6}$$

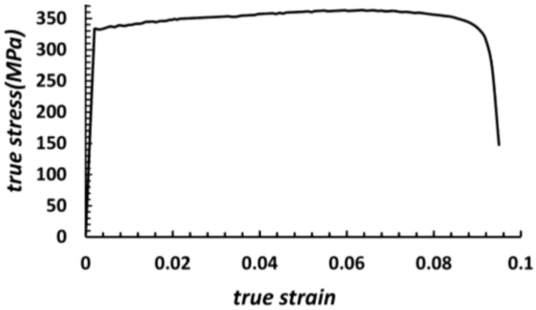

Fig. 4 True stress–strain curve for steel (substrate and core)

Fig. 5 The tensile test setup with SANTAM machine

$$SEA = \frac{E_a}{W_m} \tag{7}$$

2.1 Material properties

High-strength steel was used for absorbers. The expanded metal sheets were constructed using a cold-rolled ASTM A-611 steel (ASTM Int. 2000). The material characteristics were obtained from the standard tensile tests ASTM E08M-04 (ASTM Int. 2009) on the specimens directly cut from the sheets. The tensile test curve is shown in Fig. 4. Tensile tests were carried out in order to determine the mechanical properties of the cores and sheets as shown in Fig. 5. The material properties are shown in Table 2.

2.2 Design of experiments

The aim of design of experiments (DOE) techniques is to provide approximated response surfaces that are sufficiently accurate to replace the true response and can be used to facilitate design space exploration. Box-Behnken designs (BBD) are response surface designs, specially made to require only 3 levels, coded as -1, 0, and +1. BBD are available for 3 to 10 factors. They are formed by combining two-level factorial designs with incomplete block designs. This procedure creates designs with desirable statistical properties but, most importantly, with only a fraction of the

Table 2 The material properties

s_y (MPa)	s_u (MPa)	E (MPa)	r (kg/m^3)	u
333.52	363.47	201	7800	0.3

Table 3 Factors and coded levels in the BBD

Levels	t_s (mm)	N (core layers number)	φ (mm^2)
-1	1	3	0.081
0	2	6	0.145
1	3	9	0.562

experiments required for a three-level factorial. Because there are only three levels, the quadratic model is appropriate.

Characteristics of the BBD In many scientific studies that require RSM, researchers are inclined to require three evenly spaced levels (Borges *et al*. 2016). Thus, the BBD is an efficient option and indeed an important alternative to the central composite design (Myers *et al*. 2016). The encoded values are calculated using Eq. (8).

$$x_i = \frac{X_i - X_0}{\Delta X_i} \tag{8}$$

Where x_i is the value marked for the independent variable, X_i is the real value of the independent variable, X_0 is the real value of the independent variable at the center point, and 2 divide ΔXi (variable at high surface-variable at the low surface). The polynomial equation of the second-order regression model is shown in Eq. (9) (Chen *et al*. 2006) to express the predictive response (Y) as a function of independent variables

$$Y = \beta_0 + \sum_{i=1}^{k} \beta_i x_i + \sum_{i=1}^{k} \beta_{ii} (x_i)^2 + \sum_{i=1}^{k-1} \sum_{j=2}^{k} \beta_{ij} x_i x_j \tag{9}$$

Where β_0, β_i, β_{ii}, β_{ij}, are regression coefficients. β_i is the linear effect term, β_{ii} is the square effect term, β_{ij} is the interaction effect term (β_0 is a fixed term related to the response). x_i and x_j are the variables indicating important and effective parameters in the process.

In the analysis, three factors are chosen with three levels each: size of the cell, (Factor 1); core layers number, N (Factor 2), and the thickness of top and bottom substrates, t_s (Factor 3). Table 3 presents the values corresponding to low, mid and high coded levels in the BBD for the three investigated factors. Center points are repeated 3 times to get a good estimate of experimental error (pure error). At this stage, it is important to mention that the resulting model for the response is only valid within the ranges of the factors. The 15 runs combinations for the BBD are shown in Table 4.

Table 4 Computational design of experiments

Run	Specimen	Factor		
		φ (mm^2)	N (core layers number)	t_s (mm)
1	C132	0.081	3	2
2	C192	0.081	9	2
3	C332	0.562	3	2
4	C392	0.562	9	2
5	C231	0.145	3	1
6	C291	0.145	9	1
7	C233	0.145	3	3
8	C293	0.145	9	3
9	C161	0.081	6	1
10	C361	0.562	6	1
11	C163	0.081	6	3
12	C363	0.562	6	3
13	C262.1	0.145	6	2
14	C262.2	0.145	6	2
15	C262.3	0.145	6	2

3. Experimental setup

The specimens were made based on the parameters obtained from the DOE (see Fig. 6). The substrates and core layers are spots welded to one another along both ends of the surfaces in contact. Label model indicated in Table 4.

Quasi-static tests at a constant speed of 10 mm/min were conducted on sandwich beams by using SANTAM-stm 400 machine (see Fig. 7). During the tests, the central deflection of the front face and the corresponding load on the structure was recorded. Fig. 8 shows the deformation progress of a sandwich beam with lattice core. Force-displacement and energy-displacement curves for the sandwich beam with three different cores are shown in Fig. 9.

4. Numerical simulation

Finite element analysis was conducted by using ABAQUS/EXPLICT (Abaqus 2014), for simply supported sandwich beams under quasi-static compressive loading. As

Fig. 6 Specimens were made based on the parameters obtained from the DOE

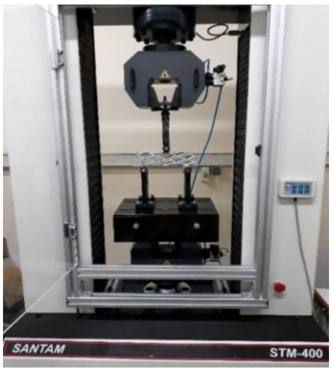

Fig. 7 The experimental setup

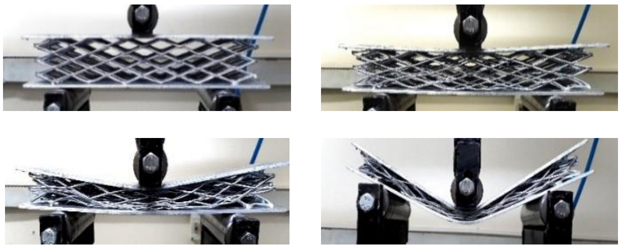

Fig. 8 Photographs of specimen c293 during test

shown in Fig. 10, due to the symmetry of the beam structures, the rest of the samples were half-modeled to reduce the computational time. The substrate was meshed with C3D8I elements. The C3D8I element is the first-order fully integrated three-dimensional 8-node solid element, enhanced by incompatible modes to improve its bending behavior.

The element used for modeling the lattice cores was S4R 4-node thick shell. Fig. 11 shows a typical mesh for an expanded metal cell. The support and punch were modeled as rigid shells meshed with discrete rigid elements (element type R3D4). True stress against true plastic strain curves was used in the FEA, which was converted from the engineering stress–strain curves obtained in the tensile tests. The punch had a single degree of freedom (DOF) in the direction normal to the plane of the top substrate, while all other DOFs of the punch were constrained.

To apply the friction between the constituents in the simulation, the penalty friction formulations were used. The contact interactions between the bottom substrate and rigid support, and between the top substrate and punch were modeled as the “surface to surface” contact was defined with the friction coefficient of 0.25 (Najibi *et al.* 2016, Sun *et al.* 2017, Tarlochan *et al.* 2013). A “self-contact” interface was also selected to simulate the collapse of the

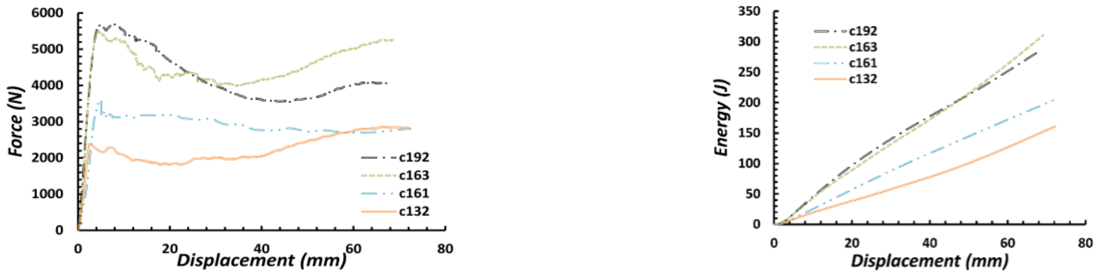

(a)

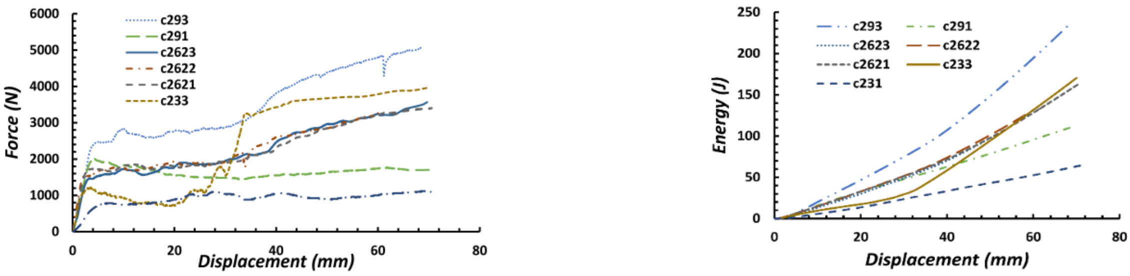

(b)

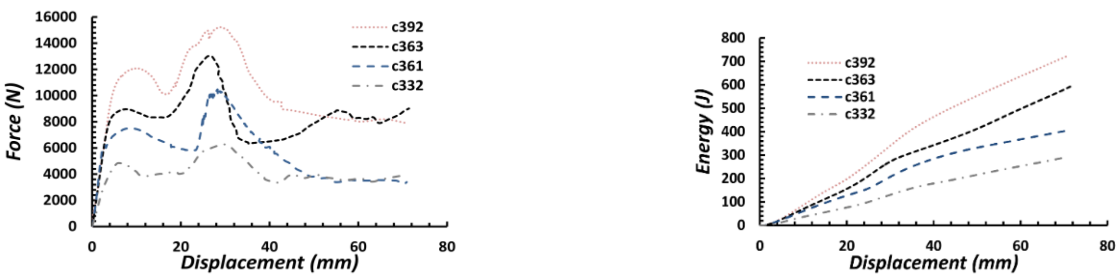

(c)

Fig. 9 Load-displacement response and energy-displacement curve for sandwich beam with three different cores by: (a) $\varphi = 0.081$; (b) $\varphi = 0.145$; (c) $\varphi = 0.562$

(a) (b)

Fig. 10 (a) FEM model; (b) boundary condition and loaded area

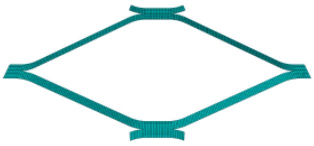

Fig. 11 Mesh for an expanded metal cell

specimens when the elements of the lattice core contacted each other.

To study the mesh sensitivity, three cases of different mesh size were analyzed for the model of a sandwich beam. For the elastic deformation, the curves from the three cases were almost the same. For the stage of plastic deformation, cases 2 and 3 demonstrated similar results, indicating that the mesh size of 1 mm was sufficiently optimal. The simulation results in terms of force–displacement curves are compared in Fig. 12.

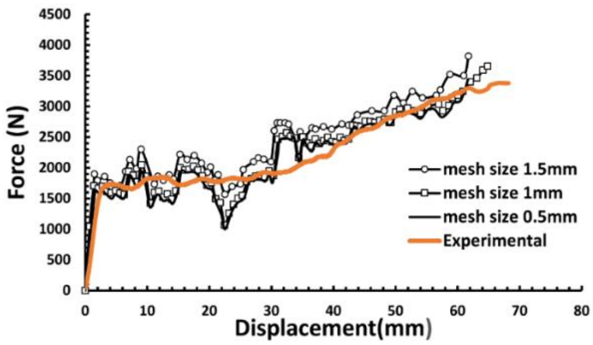

Fig. 12 Validation of mesh size for finite element simulation (c262 specimen)

5. Results and discussion

It is noted that the crushing of the sandwich beam with a core of type φ = 0.145 mm^2 arrangement began at a relatively small load of 2300 N, and the bending of the beam was not obvious in the early stages of the test. In agreement with our experimental observations, the deformed shapes predicted in the early stages of our FE simulation also showed core crushing as the major deformation mode.

During the quasi-static tests, it is also noted that when the crushing of the core was nearly complete, the entire beam began to bend in this kind of cores. During the tests on the sandwich beam with core types of φ = 0.562 mm^2, it is observed that the onset of core crushing occurred at a much higher load of 11000 N, due to the greater thickness of the core layers. In this core types after the one cell of the lattice sheet was crushed, the core compression and bending phases were coupled. For all the beams, there exists an initial stage of linear elastic deformation. Afterwards, plastic deformation occurs, where the load increases

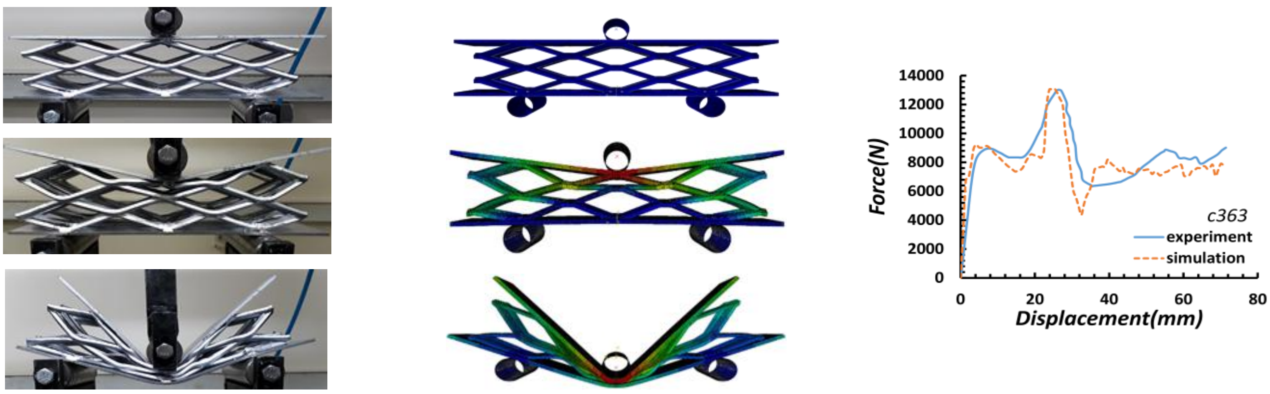

(a) (b) (c)

Fig. 13 Comparison of the experiments and FEA predications for the mechanical response of the sandwich beam with lattice core bending deformation: (a) experimentally deformed specimens; (b) corresponding simulated FEA results; and (c) force-displacement curves for c363

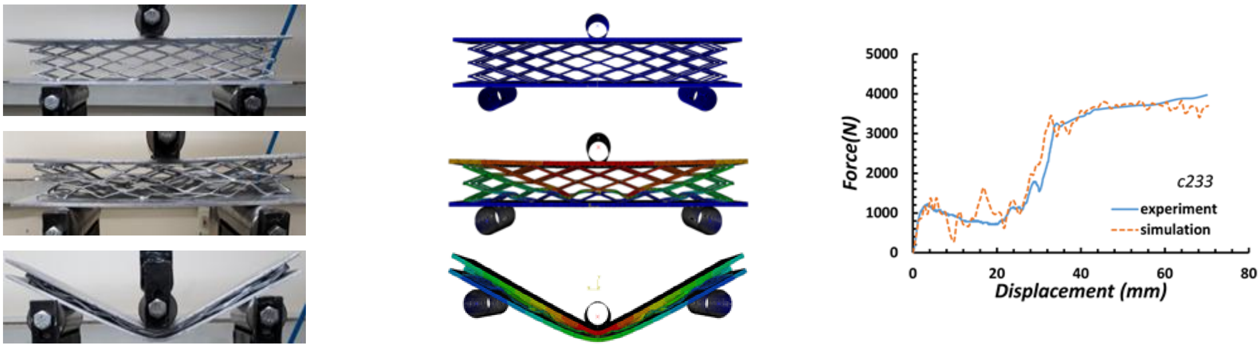

(a) (b) (c)

Fig. 14 Comparison of the experiments and FEA predications for the mechanical response of the sandwichbeam with lattice core bending deformation: (a) experimentally deformed specimens; (b) corresponding simulated FEA results; and (c) force-displacement curves for c233

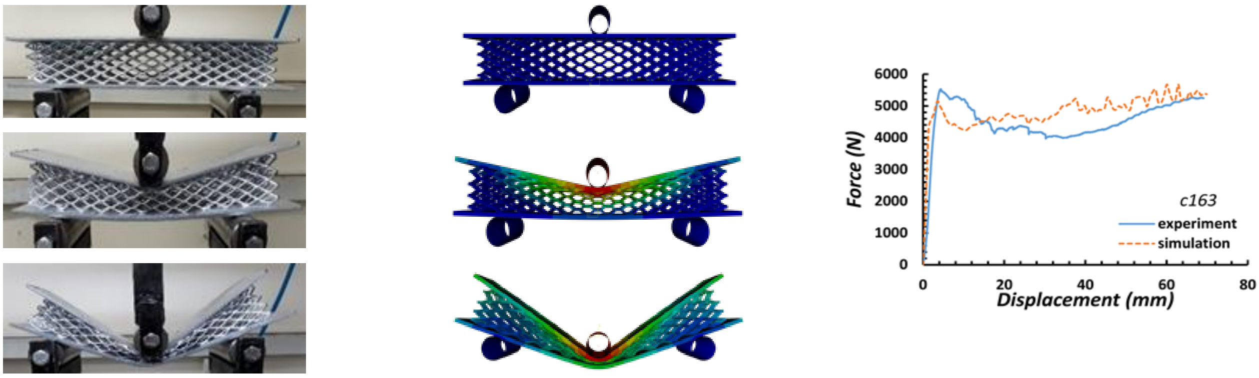

(a) (b) (c)

Fig. 15 Comparison of the experiments and FEA predications for the mechanical response of the sandwich beam with lattice core bending deformation. (a) experimentally deformed specimens; (b) corresponding simulated FEA results; and (c) force-displacement curves for c163

gradually with the displacement.

Results showed that force-displacement curves achieved by numerical simulations were in good agreement with those obtained from the experimental tests. Nevertheless, little disagreement between the simulation and experimental results can be attributed to the fact that our simulation model does not clear for the effects of initial material imperfections in the core layers and the imperfect connection between the sandwich beam components.

In the quasi-static tests, it is observed that the welds joining the substrates to the core layers, as well as those joining the core layers to one another, were in general frailer than the rest of the structure, and the connection did occur in a few cases. The performed tests and the force-displacement curves of the models are shown in Figs. 13-16. The experimental load-deflection behavior of each core arrangement is compared with finite element results (see Fig. 16).

Their force-displacement curves had relatively regular oscillations considering the type of the core. The data found from the curves showed that the peak force was suitable and was close to the mean force. The calculated energy absorption showed this too. The energy absorption capacities were calculated for all models. The absorbed energy obtained numerically and experimentally was then compared. (See Table 5).

The experiments showed that sandwich beam with thicker substrates had a more homogeneous collapsed in the longitudinal direction of the beam.

The energy absorption capacity of all the tested beams at the same deflection of 68 mm was evaluated by the energy absorption (E_a) and specific energy absorption (SEA), as illustrated in Fig. 17. It is clear from this figure that the sandwich specimen of C392 has the highest SEA is equal to 729.82 J/kg.

For the specimens studied in this research work, all the specimens displayed good progressive deformation. From this figure, it can be seen that the least value of the absorbed energy in those specimens was 64.154 J belonging to c231 with a decrease between 41% and 91% with respect to the sandwich specimens. The largest value of the absorbed energy was 720.62 J belonging to the sandwich specimen C392, which was 91% greater than that of c231.

For the sandwich beams with lattice core, energy absorption was calculated from both the analytical method and FE simulation. The contribution of each specimen to the energy absorption is given in Fig. 18.

Experimental tests require time and money, and therefore, can be replaced by numerical simulations. Results showed that energy absorption values obtained by the

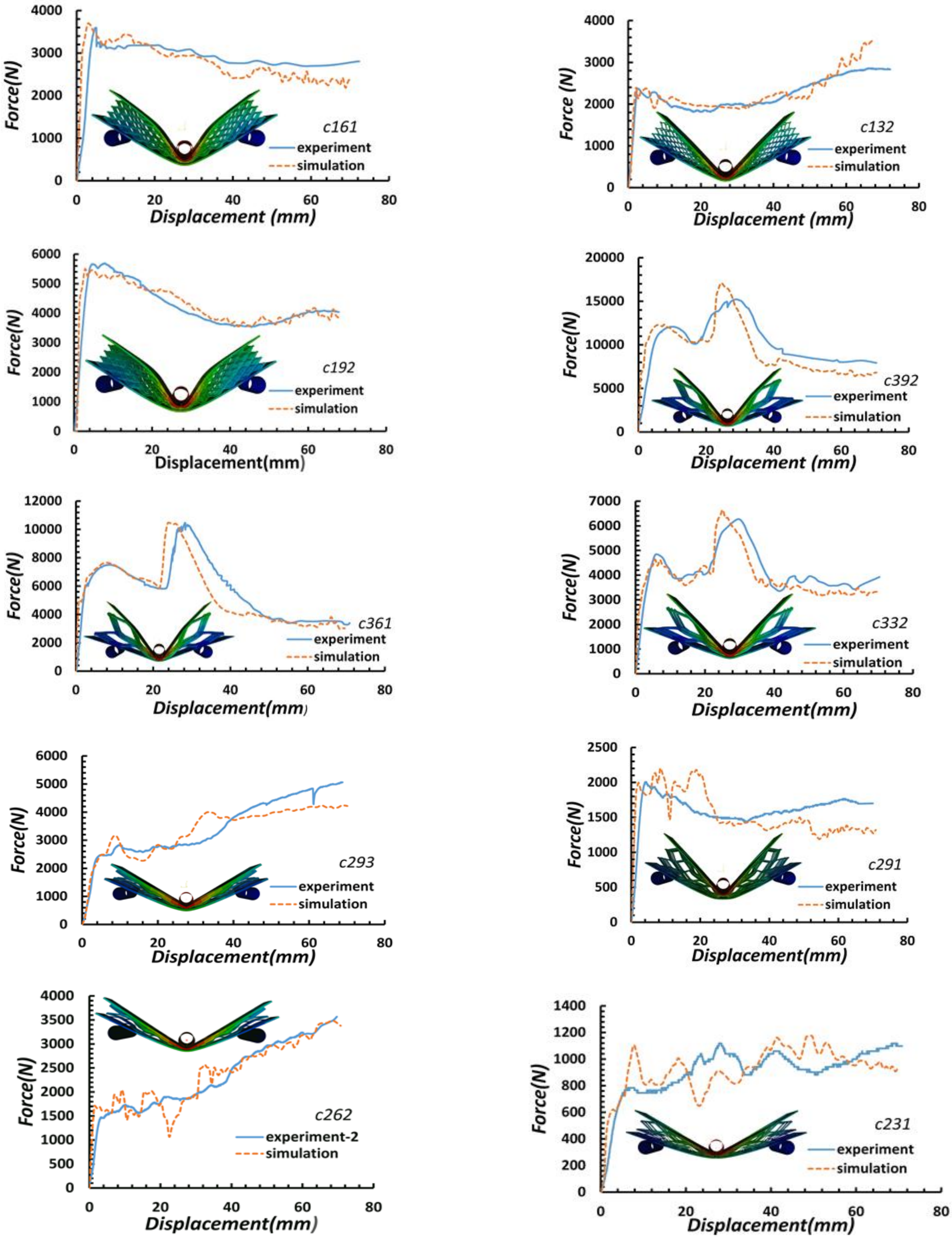

Fig. 16 Comparison of the experiments and FEA predictions force-displacement curves for all sandwich beams

numerical simulations were in good agreement with those obtained from the experimental tests. As can be seen, and also as already mentioned, the values were to some extent consistent with each other; however, errors were observed in some cases.

Fig. 19 shows the experimental results for the crush force efficiency. As is evident from this figure, the least value of the crush force efficiency was 65.9% and 68.5% belonged to the specimens C332 and C161, respectively. However, the largest value of the crush force efficiency in the experimental specimens was 143.88% belonging to the specimen C262.2. This is due to the fact that the peak load was smaller than the mean crush load in those specimens. Comparing the peak loads, the highest values corresponded

Table 5 Experimental and numerical results of specimens

Specimen	W_m (kg)	P_{mean} (N)	P_{Peak} (N)	E_a^{Sim} (J)	E_a^{Exp} (J)	Error (%)	SEA(J/kg)	CFE (%)
C132	0.48	2233.16	2378.87	153.921	160.795	-4.27	331.5	93.874
C192	0.57	4177.7	5667	287.943	283.573	1.54	495.29	73.719
C332	0.62	3188.6	4833.6	277.443	290.782	-4.58	463.99	65.968
C392	0.98	11553.26	12075.5	670.228	720.62	-6.99	729.8	95.675
C231	0.33	906	784	64.134	64.154	-0.03	191.5	115.571
C291	0.407	1605	1991.5	109.318	112.742	-3.03	276.69	80.594
C233	0.67	1177.4	1202.5	174.811	170.333	2.62	253.3	97.914
C293	0.74	3454.6	2466.4	235.622	237.802	-0.91	319.07	140.067
C161	0.404	2419	3528.78	194.064	205.83	-5.71	508.69	68.552
C361	0.63	7516.65	7587.71	383.507	405.345	-5.38	637.47	99.063
C163	0.74	4494.96	5528.5	337.116	310.711	8.49	418.91	81.304
C363	1.003	7527.26	8937	558.39	592.529	-5.76	590.54	84.225
C262.1	0.51	2167.4	1722	166.093	162.873	1.97	318.63	125.867
C262.2	0.51	2201.38	1530	166.093	163.81	1.39	320.95	143.881
C262.3	0.508	2143.7	1575	166.093	160.464	3.50	315.53	136.11

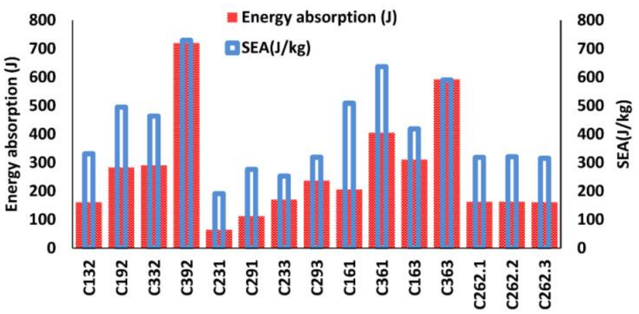

Fig. 17 Comparison of total energy absorbed and SEA between specimens

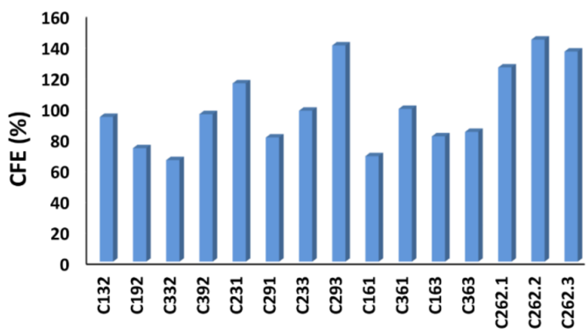

Fig. 19 Comparison of crush force efficiency between specimens

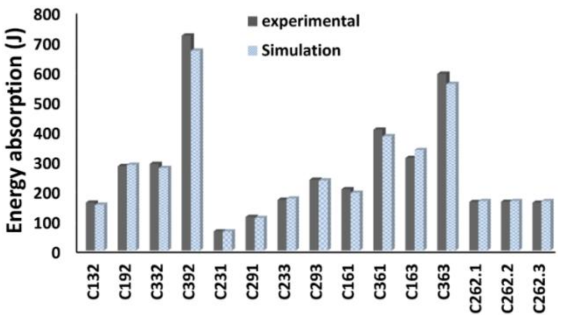

Fig. 18 Energy absorption for sandwich beams, from the FE simulation and experimental test

to the sandwich beam with type core of φ = 0.562 mm^2, In general, these cores are more efficient than other cores.

5.1 Parametric study on a structural beam

The influence of the design variables on the responses is assessed using the Design-Expert software. In order to study the Sensitivity factors, the analysis of variance (ANOVA) has been conducted (Das and Mishra 2017).

In the examination of the model, the sum of squares (SS), and the mean sum of squares (MS) are calculated by measuring responses. In this analysis, there are two parameters named F-value and P-value. F-value denotes the ratio of the MS to MS error, and P-value indicates the significance of a factor. P-value = 1 and P-value = 0 correspond to the smallest and greatest important factor, respectively. In the RSM model terms with P-value < 0.05 can be used in predicting the behavior of response, so they are conserved in the mathematical model.

5.1.1 Specific energy absorption

Table 6 represents the ANOVA results for specific energy absorption. The Model F-value of 49.16 implies the model is significant. There is only a 0.01% chance that a "Model F-value" this large could occur due to noise. Values of "Prob > F" less than 0.05 indicate model terms are significant. In this case, N, φ, N^2, φ^2 are significant model terms.

The "Lack of Fit F-value" of 174.77 implies the lack of fit is significant. There is only a 0.57% chance that a "Lack of Fit F-value" this large could occur due to noise. Significant lack of fit is bad. We want the model to fit. The

Table 6 Analysis of variance (ANOVA) table for SEA - quadratic model

Source	Sum of squares	df	Mean square	F-value	P-value
Model	0.41	4	0.10	49.16	< 0.0001
N-core layers	0.057	1	0.057	27.33	0.0004
φ-cell size	0.050	1	0.050	23.97	0.0006
N^2	0.017	1	0.017	8.03	0.0178
φ^2	0.14	1	0.14	65.34	< 0.0001
Residual	0.021	10	2.096E-003		
Lack of fit	0.021	8	2.616E-003	174.77	0.0057
Pure error	2.994E-005	2	1.497E-005		
Cor total	0.43	14			
R-squared	0.9516				
Adj R-squared	0.9323				
Pred R-squared	0.8901				

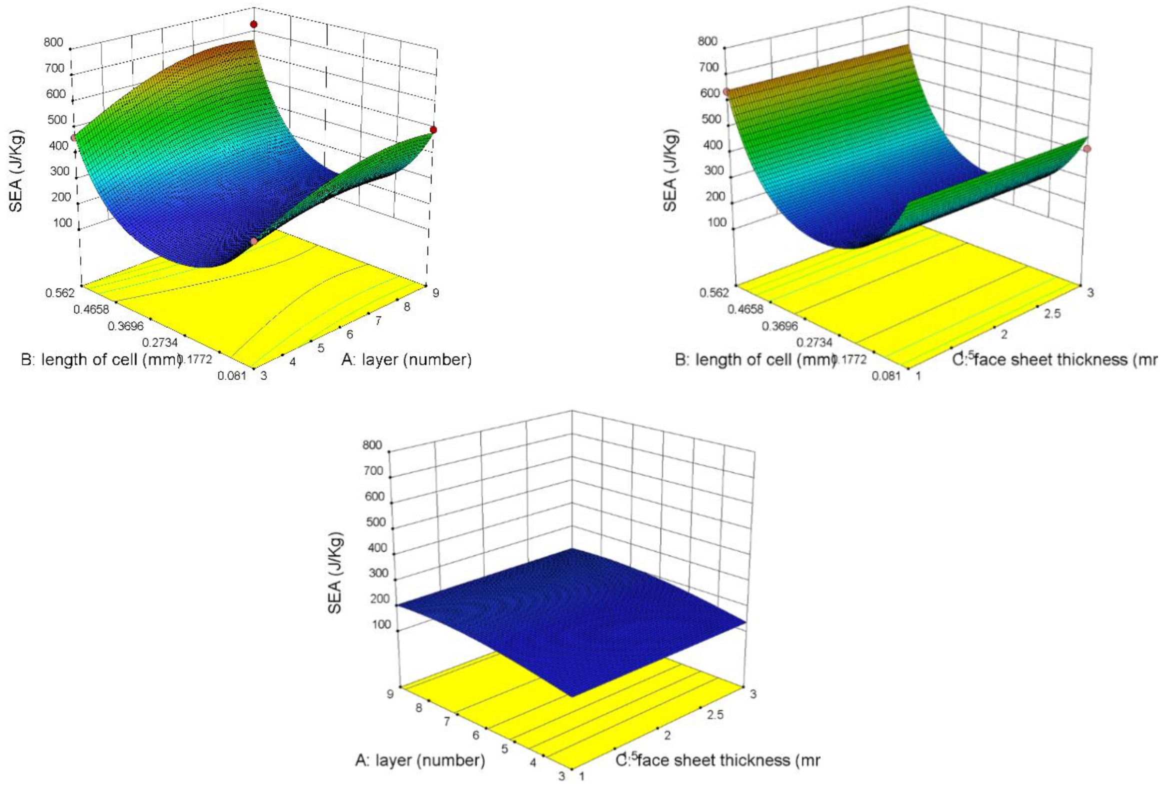

Fig. 20 The interaction effects of independent variables on SEA

amount of R-square is equal to 0.9516, which means that 95.16% of the variation in the SEA is predictable by the core layers number, size of the cell and thickness of substrates. Eq. (10) is the final equation in terms of actual factors for indicates the predictability of the variations in the SEA obtained by Quadratic model.

$$(SEA)0.17 = 2.74209 + 0.11793 \times N - 4.84285 \times \varphi - 7.47737 \times 10^{-3} \times N^2 + 8.04410 \times \varphi^2 \quad (10)$$

In this equation, N is core layers number and, φ is the size of the cell. The high value of P-value for the thickness of substrates reveals that there is not enough reason to accept the effect of thickness of substrates on the SEA in the conducted study.

To compare the effect of all the factors at a particular point (midpoint (coded 0) of all the factors) (Sheriff *et al*. 2008) in the design space, the three-dimensional plots of SEA model vs. each independent variable are illustrated in Fig. 20.

5.1.2 Peak force

Table 7 presents the ANOVA results for P_{peak}. The Model F-value of 269.94 implies the model is significant.

Table 7 Analysis of variance (ANOVA) table for P_{peak}- quadratic model

Source	Sum of squares	df	Mean square	F-value	P-value
Model	0.31	5	0.063	269.94	< 0.0001
N-layer	0.050	1	0.050	215.79	< 0.0001
φ-length of cell	0.035	1	0.035	151.33	< 0.0001
t_s-face sheet thickness	6.565E-003	1	6.565E-003	28.22	0.0005
N^2	1.390E-003	1	1.390E-003	5.97	0.0371
φ^2	0.11	1	0.11	475.93	< 0.0001
Residual	2.094E-003	9	2.327E-004		
Lack of fit	1.861E-003	7	2.659E-004	2.28	0.3380
Pure error	2.328E-004	2	1.164E-004		
Cor total	0.32	14			
Model	0.31	5	0.063	269.94	< 0.0001
R-squared	0.9934				
Adj R-squared	0.9897				
Pred R-squared	0.9799				

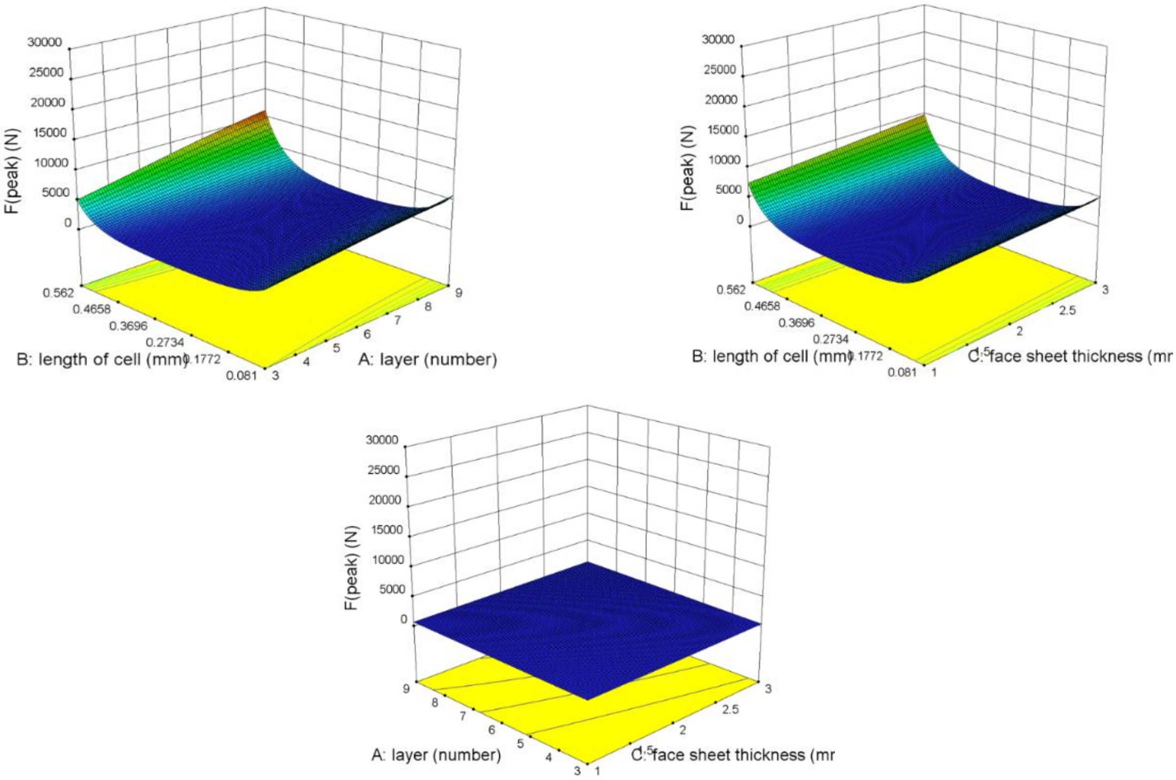

Fig. 21The interaction effects of independent variables on P_{peak}

There is only a 0.01% chance that an "F-Value" this large could occur due to noise. Values of "Prob > F" less than 0.05 indicate model terms are significant. In this case, $N, \varphi, t_s, N^2, \varphi^2$ are significant model terms. Values greater than 0.1000 indicate the model terms are not significant. The "Lack of Fit F-value" of 2.28 implies the lack of fit is not significant relative to the pure error. There is a 33.80% chance that a "Lack of Fit F-value" this large could occur due to noise. Nonsignificant lack of fit is good. We want the model to fit.

The response surface equation for peak force is given in Eq. (11).

$$(P_{peak})^{0.09} = 2.13540 + 0.052198 \times N - 4.37536 \times \varphi + 0.028647 \times t_s - 2.14927 \times 10^{-3} \times N^2 + 7.23360 \times \varphi^2 \tag{11}$$

In this equation, N is core layers number, φ is the size

Table 8 Analysis of variance (ANOVA) table for CFE - quadratic model

Design variable			P_{peak}	SEA
N	φ (mm^2)	t_s (mm)		
5.87	0.5411	1	4874.08	99.65

of the cell and, t_s is the thickness of substrates three-dimensional surface plots in Fig. 21; represent the P_{peak} the other two variables indicated on each graph.

In this study, the optimum values for design variables are obtained from Design-Expert software. In this software, the optimization method is started by applying the upper and lower limit of design variables and defining the aim of optimization. As in Eq. (12), here, the optimization is realized based on maximizing the objective functions of specific energy absorption and minimize peak force. Considering the same importance for two objective functions, the optimum values for variables and the consistent responses are provided in Table 8.

6. Conclusions

In the present study, three-point bending experiments of the sandwich beams with expanded metal sheets as core have been conducted. Quasi-static compressive loading tests were conducted on sandwich beams. The relationship between the force and displacement at the middle point of the sandwich beam was obtained from the experiments. Moreover, Bending collapse mechanisms for the beams with different cores were analyzed.

The simulation was performed using ABAQUS. The results of the experimental tests and numerical simulations, as well as the collapse shapes of the models, showed that the sandwich beam with lattice cores can be used as energy absorbers in the industry.

A parametric study was conducted using a BBD to investigate the influence of the core layers number, size of the cell and, the thickness of substrates. From the viewpoint of the sandwich beams design, influence of design parameters on the objectives discovered through regression model and optimum values for design parameters are determined.

In the present research, for the first time, when these sandwich beams were subjected to quasi-static three-point bending, it was found that contrary to their low weight, the sandwich beams can absorb the clash energy due to their mesh and multiple joints and nodes in the core. The major conclusions are summarized as follows:

- Introducing higher size of the cell core in sandwich beams does not necessarily give higher energy absorption efficiency. Increasing the cell size in a reasonable range is required to improve the performance of the structure under bending collapse.
- It was revealed that the core layers number and the size of the cell affect the SEA in the mentioned order. Also the core layers number, size of the cell and, thickness of substrates, all influence CFE in the mentioned order.
- The maximum CFE was accrued in the higher core layers number, thickness of substrates and lower size of the cell core. Moreover, the maximum SEA was observed in the higher core layers number and highest and lowest amount of cell size.
- The results showed that the size of the cells is the most influential parameter to increase mean and peak forces. Expanded metal sheets have a symmetric collapse mechanism due to their structure. This resulted in a good order force-displacement curve. The peak force was low and close to the average force, even in some cases, it has been less. The calculation of the crushing force efficiency also indicated this matter. The calculated crushing force efficiency showed that the sandwich beam with lattice core had a high efficiency of energy absorption.
- Sandwich beams with expanded metal sheets as the core can be used in industry as a modern absorber. This is because, despite their very low weight, such beams can endure symmetric collapse under quasi-static loading and crush to their ends.

Finally, the results showed that DOE techniques, experimental testing, and finite element modeling are dependable tools to investigate the energy absorption response of sandwich beam with lattice core.

References

Abaqus (2014), Abaqus analysis user's manual, Dassault Simulia, Version 6.14.

ASTM Int. (2000), Standard Specification for Steel, Sheet, Carbon, and High-Strength, Low-Alloy, Hot-rolled and Cold-rolled, ASTM. (A 568/A 568M)

ASTM Int. (2009), Standard Test Methods for Tension Testing of Metallic Materials, ASTM, (C), pp.1-27.

Borges, H., Martínez, G. and Graciano, C. (2016), "Impact response of expanded metal tubes: A numerical investigation", *Thin-Wall. Struct.*, **105**, 71-80.

Chen, V.C., Tsui, K.L., Barton, R.R. and Meckesheimer, M. (2006), "A review on design, modeling and applications of computer experiments", *IIE Transactions*, **38**(4), 273-291.

Crupi, V. and Montanini, R. (2007), "Aluminium foam sandwiches collapse modes under static and dynamic three-point bending", *Int. J. Impact Eng.*, **34**(3), 509-521.

Daniel, I.M., Gdoutos, E.E., Abot, J.L. and Wang, K.A. (2003), "Deformation and failure of composite sandwich structures", *J. Thermopl. Compos. Mater.*, **16**(2), 345-355.

Daniel, I.M., Gdoutos, E.E., Wang, K.A. and Abot, J.L. (2002), "Failure Modes of Composite Sandwich Beams", *Int. J. Damage Mech.*, **11**(4), 309-334.

Das, S. and Mishra, S. (2017), "Box-Behnken statistical design to optimize preparation of activated carbon from Limonia acidissima shell with desirability approach", *J. Environ. Chem. Eng.*, **5**(1), 588-600.

Gibson, L.J. and Ashby, M.F. (1997), *Cellular Solids*: *Structure and Properties*, (2nd Ed.), Cambridge University Press, Cambridge, UK.

Graciano, C., Martínez, G. and Gutiérrez, A. (2012), "Failure mechanism of expanded metal tubes under axial crushing", *Thin-Wall. Struct.*, **51**, 20-24.

Graciano, C., Martínez, G. and Smith, D. (2009), "Experimental investigation on the axial collapse of expanded metal tubes", *Thin-Wall. Struct.*, **47**(8-9), 953-961.

Hatami, H. and Damghani Nouri, M. (2015), "Experimental and numerical investigation of lattice-walled cylindrical shell under low axial impact velocities", *Latin Am. J. Solids Struct.*, **12**(10), 1950-1971.

Hu, Y., Li, W., An, X. and Fan, H. (2016), "Fabrication and mechanical behaviors of corrugated lattice truss composite sandwich panels", *Compos. Sci. Technol.*, **125**, 114-122.

Hyun, S., Karlsson, A.M., Torquato, S. and Evans, A.G. (2003), "Simulated properties of Kagome and tetragonal truss core panels", *Int. J. Solids Struct.*, **40**(25), 6989-6998.

Jahromi, A.G. and Hatami, H. (2017), "Energy absorption performance on multilayer expanded metal tubes under axial impact", *Thin-Wall. Struct.*, **116**, 1-11.

Kooistra, G.W. and Wadley, H.N.G. (2007), "Lattice truss structures from expanded metal sheet", *Mater. Des.*, **28**(2), 507-514.

Li, Q.M., Ma, G.W. and Ye, Z.Q. (2006), "An elastic–plastic model on the dynamic response of composite sandwich beams subjected to mass impact", *Compos. Struct.*, **72**(1), 1-9.

Sheriff, N.M., Gupta, N.K., Velmurugan, R. and Shanmugapriyan, N. (2008), "Optimization of thin conical frusta for impact energy absorption", *Thin-Wall. Struct.*, **46**(6), 653-666.

Myers, R.H., Montgomery, D.C. and Anderson-Cook, C.M. (2016), *Response Surface Methodology: Process and Product Optimization Using Designed Experiments*, John Wiley and Sons, (4th Edition).

Najibi, A., Shojaeefard, M.H. and Yeganeh, M. (2016), "Developing and multi-objective optimization of a combined energy absorber structure using polynomial neural networks and evolutionary algorithms", *Latin Am. J. Solids Struct.*, **13**(14), 2252-2272.

Nouri, M.D., Hatami, H. and Jahromi, A.G. (2015), "Experimental and numerical investigation of expanded metal tube absorber under axial impact loading", *Struct. Eng. Mech., Int. J.*, **54**(6), 1245-1266.

Pedersen, C.B.W., Deshpande, V.S. and Fleck, N.A. (2006), "Compressive response of the Y-shaped sandwich core", *Eur. J. Mech., A/Solids*, **25**(1), 125-141.

Smith, D., Graciano, C. and Martínez, G. (2009), Recent Patents on Expanded Metal; *Recent Patents on Materials Science*, **2**, 209-225.

Smith, D.J., Graciano, C.A., Teixeira, P., Martínez, G. and Pertuz, A. (2016), "Energy absorption characteristics of coiled expanded metal tubes under axial compression", *Latin Am. J. Solids Struct.*, **13**(16), 2845-2860.

Sun, G., Pang, T., Xu, C., Zheng, G. and Song, J. (2017), "Energy absorption mechanics for variable thickness thin-walled structures", *Thin-Wall. Struct.*, **118**, 214-228.

Tarlochan, F., Samer, F., Hamouda, A.M.S., Ramesh, S. and Khalid, K. (2013), "Design of thin wall structures for energy absorption applications: Enhancement of crash-worthiness due to axial and oblique impact forces", *Thin-Wall. Struct.*, **71**, 7-17.

Teixeira, P., Martínez, G. and Graciano, C. (2016), "Shear response of expanded metal panels", *Eng. Struct.*, **106**, 261-272.

Vaidya, S., Zhang, L., Maddala, D., Hebert, R., Wright, J.T., Shukla, A. and Kim, J.H. (2015), "Quasi-static response of sandwich steel beams with corrugated cores", *Eng. Struct.*, **97**, 80-89.

Xiang, X.M., Lu, G. and Wang, Z.H. (2015), "Quasi-static bending behavior of sandwich beams with thin-walled tubes as core", *Int. J. Mech. Sci.*, **103**, 55-62.

Zhu, F., Lu, G., Ruan, D. and Wang, Z. (2010), "Plastic deformation, failure and energy absorption of sandwich structures with metallic cellular cores", *Int. J. Protect. Struct.*, **1**(4), 507-541.

CC